Assessing Cold-Snap and Mortality Events in South Florida Coastal Ecosystems: Development of a Biological Cold Stress Index Using Satellite SST and Weather Pattern Forcing

Douglas E. Pirhalla, Scott C. Sheridan, Varis Ransibrahmanakul & Cameron C. Lee

Estuaries and Coasts
Journal of the Coastal and Estuarine Research Federation

ISSN 1559-2723
Volume 38
Number 6

Estuaries and Coasts (2015)
38:2310-2322
DOI 10.1007/s12237-014-9918-y

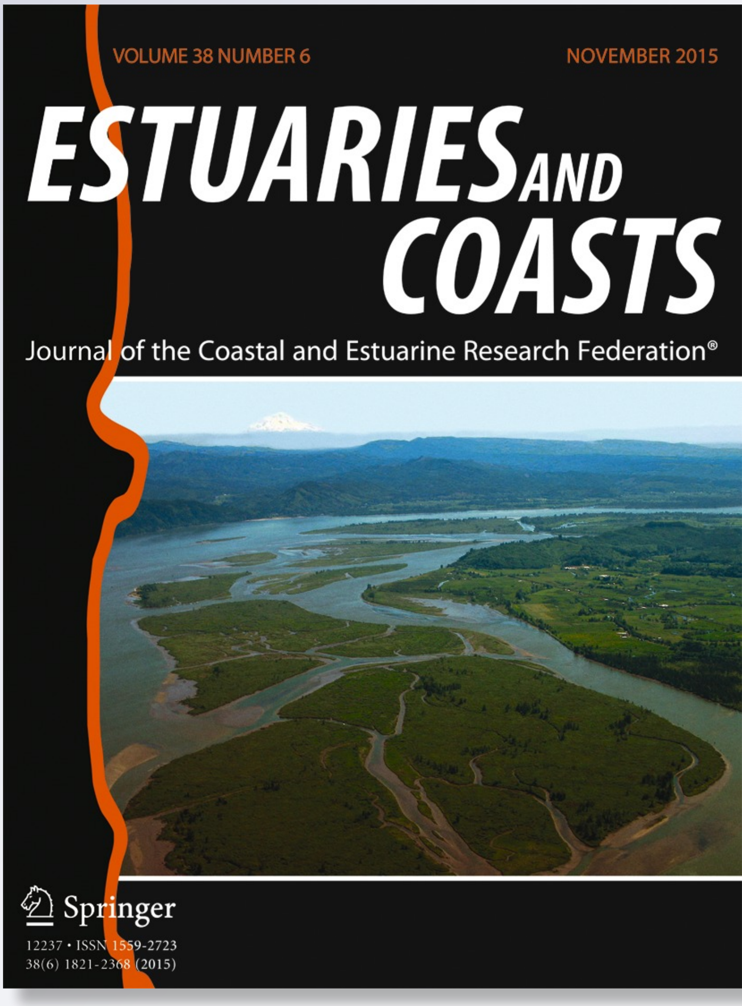

Springer

Estuaries and Coasts (2015) 38:2310–2322
DOI 10.1007/s12237-014-9918-y

Assessing Cold-Snap and Mortality Events in South Florida Coastal Ecosystems: Development of a Biological Cold Stress Index Using Satellite SST and Weather Pattern Forcing

Douglas E. Pirhalla · Scott C. Sheridan · Varis Ransibrahmanakul · Cameron C. Lee

Received: 8 July 2014 / Revised: 7 November 2014 / Accepted: 13 November 2014 / Published online: 3 December 2014

Abstract Water temperature is considered both a controlling and lethal factor in coastal ecosystems, influencing behavioral and physiological responses in marine organisms. Abrupt weather events such as severe cold front passages and accompanied changes in weather conditions have led to sharp decreases in water temperatures, metabolic stress, and incidences of mortality in marine organisms. In this paper, we assess the weather-related factors associated with physical and biological response in South Florida systems through historical sea surface temperature (SST) from satellites and the use of a synoptic climatology spanning over 30 years. We utilize previous categorizations of sea-level pressure and newly developed categorizations of 850-mb temperature reanalysis data to define circulation and temperature patterns across the southeastern US and adjacent Gulf of Mexico. Systematic connections are seen between particular circulation and temperature patterns characteristic of enhanced north-to-south circulation and cold air outbreaks, SST, and turtle strandings data over the Florida Panhandle region for the period 2006–2013. Identified weather forcing variables associated with sharp SST decreases and turtle stuns are presented and assist in the formulation of a moving cold-stress index for South Florida coastal ecosystems. Results demonstrate the potential of using synoptic climatological analysis and derived indices for tracking and modeling changes in SST and other indicators related to biological health.

Communicated by Mark J. Brush

D. E. Pirhalla (✉) · V. Ransibrahmanakul
National Center for Coastal Ocean Science, National Oceanic and Atmospheric Administration, Silver Spring, MD 20910, USA
e-mail: doug.pirhalla@noaa.gov

S. C. Sheridan · C. C. Lee
Department of Geography, Kent State University, Kent, OH 44242, USA

Keywords Sea surface temperature · Cold-snap mortality events · Synoptic climatology · Atmospheric circulation · Florida · Blended microwave/IR SST

Introduction

Water temperature is a key environmental factor and controlling variable in coastal marine ecosystems, influencing photosynthesis, dissolved oxygen levels, and metabolic and growth rates in marine organisms and how organisms respond to various pollutants, parasites, and pathogens (Fry 1971; Portner 2002; Hare et al. 2012). Temperature is also considered a lethal response factor when assessing climate variability and change impacts in systems. In particular, South Florida's economically and aesthetically important coastal resources—including fish, turtles, crustaceans, coral reefs, and their habitats—have been particularly susceptible to both gradual and abrupt (extreme) shifts in temperature, with effects ranging from severe bleaching, metabolic stress, tissue damage, and die-offs in coral species (Manzello et al. 2007; Lirman et al. 2011; Colella et al. 2012), to stress, disease, and mortality in turtles, lobsters, and manatees (Avens et al. 2012; Foley et al. 2012; Barlas et al. 2011). While gradual temperature increases leading to thermal stress and mortality in marine life (e.g., coral reef systems) are generally attributed to global-scale climatic factors (Carpenter et al. 2008; Hughes et al. 2003), acute temperature shifts are of dynamic origin, and related more to high-frequency, synoptic-scale weather phenomena coupled with complex atmospheric–oceanographic interactions and processes (Francis and Vavrus 2012; Gramer 2013; Liu and Weisberg 2007).

Variations in sea-surface temperature (SST) along the West Florida Shelf (WFS), Florida Bay, and the Florida Keys commonly result from anomalies in incoming and outgoing solar radiation, surface air–sea heating and cooling effects (e.g., latent and sensible heat fluxes), coastal upwelling, and deep water mixing (Weisberg et al. 2004; Gramer 2013). SST variations occur over a broad range of time scales, including diurnal, weekly, seasonal, and interannual duration. Causes of these variations include the passage of synoptic-scale weather systems such as cold fronts and storms during winter and tropical systems, diurnal insolation, and tidal fluctuations during summer and fall (Gramer 2013; Morey et al. 2006; Monaldo et al. 1997). For example, with a cold front passage, the entire water column in shallow coastal areas may cool by several degrees due to sensible and latent heat losses (Joyce 2002; Weisberg et al. 2004). These surface-induced changes along with upwelling-related processes, mixing, and advection are considered dominant controlling factors on short-term temperature response in this region.

Decreases in SST following cold frontal and storm passage are common during a typical winter season for the entire Gulf of Mexico (GOM) region (Wiseman and Sturges 1999). However, during an extreme and unprecedented case in January 2010, a cold air outbreak and subsequent cold-water event occurred along the entire GOM, including the Florida Reef Tract, resulting in metabolic stress, tissue damage, and widespread mortality in coral, manatee, fish, and turtle populations (Lirman et al. 2011; Colella et al. 2012; Barlas et al. 2011; Avens et al. 2012; Foley et al. 2012). Drops in air and water temperatures of 12 °C and 6 °C, respectively, were observed during January 2–17, with SST values 3–5 °C below normal throughout much of the South Florida region (Fig. 1b). The cold-water event resulted in mass numbers of turtle hypothermic cases reported (Roberts et al. 2014) and coral bleaching cases reported along Florida's coastal marine areas and estuarine environments. The event also triggered an immediate response from coral and other living marine resource management programs (e.g., Florida Reef Resilience Program, Fish and Wildlife Research Institute). Lirman et al. (2011), Foley et al. (2012), and Barlas et al. (2011) summarized the event and response, highlighting cold-water anomalies well below documented thermal tolerance *thresholds* for coral and turtle species and the Florida manatee. While relevant information exists on atmospheric variability and conditions associated with this and other extreme events (Roberts et al. 2014) and the widespread impacts from such events, a systematic understanding of the weather-related factors and underlying mechanisms associated with cold-air outbreaks and influences on SST and biota remains fairly unexplored.

One such approach to identify atmospheric factors impacting environmental response involves the use of synoptic climatological methods. Synoptic climatological methods have been applied to many environmental problems (Huth et al. 2008), including climate impact scenarios and forecasting (Sheridan et al. 2012), human health impact and heat warning systems (e.g., Sheridan and Kalkstein 2004), and, for the interpretation of associations among weather, water quality and ecosystem-level changes, and response (Sheridan et al. 2013; Kimmel et al. 2009). Sheridan et al. (2013) identified particular atmospheric circulation patterns contributing to chlorophyll response in the Gulf of Mexico, suggesting that pattern frequency, duration, and timing significantly affect the onset, diminishment, or elevation of algal bloom response and/or distribution. These methods have proven particularly applicable for coastal ecosystems where shelf- and estuarine-scale processes and air–sea fluxes are primarily controlled by weather events and not clearly linked to global-scale climate forcing (Sheridan et al. 2013; Stenseth et al. 2003).

In this study, we extend our previous work in Sheridan et al. (2013) to explore the relationship between surface weather-patterns and ocean SST climatological mean and variability along the WFS and the Florida Keys from 1981 through 2013, with emphasis on the factors associated with negative cold-season (December–March) SST anomalies and cold-snap events that have impacted the region.

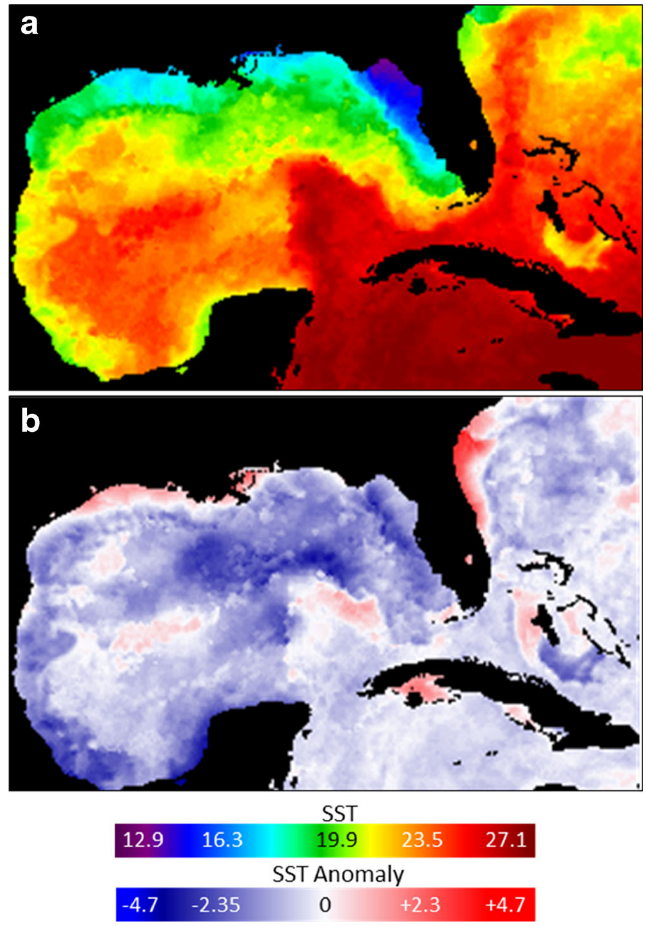

Fig. 1 Blended microwave–infrared (MW-IR) 9 km SST image for January 17, 2010, during peak of cold air outbreak and cold-stress event (**a**) and SST anomaly showing much below normal temperatures for the entire region of interest (**b**). Anomaly was calculated as the instantaneous SST for January 17, 2010, minus the long-term mean SST for January 17, normalized by SST standard deviation for January 17, for 2006 through 2013. MW-IR SST products are available from RSS, Inc. (http://www.remss.com/)

Herein, we utilize separate synoptic categorizations of two atmospheric fields from the North American Regional Reanalysis (NARR): our prior classification of anomalous mean sea-level pressure (MSLP) fields (Sheridan et al. 2013), to represent the synoptic situation, general weather conditions, and wind stress; and a classification of 850-mb temperature (T850) patterns to represent thermal conditions of the lower troposphere. These categorizations are then compared with SST and anomaly time series derived from two additional data sets: the blended multi-platform Microwave (MW)/infrared (IR) sensor product, and the Advanced Very-High-Resolution Radiometer (AVHRR) Pathfinder IR product. Systematic connections between datasets are then identified that relate frequencies of key synoptic circulation and temperature patterns to SST response, which can then be used to assess potential mechanisms that link ambient weather to SST and biological response for the region. Highlighted are the specific surface weather patterns and historical incidences related to significant drops in SST at or below documented thermal limits for turtle and coral species. Using these results, we formulate a cold-stress index (CSI), based on observed changes in SST over time. We then compare time series of CSI with frequency and severity of turtle stun events from Florida's Sea Turtle Stranding and Salvage Network and database maintained by the Florida Fish and Wildlife Conservation Commission's Fish and Wildlife Research Institute and adapted from Roberts et al. (2014). Finally, we empirically link aggregate weather patterns and frequencies to predict changes in CSI and extreme anomalous SST near lethal thermal limits based on synoptic-scale forcing. We argue that synoptic-scale approaches in modeling ecological response are reliable and applicable for most marine organisms impacted by weather-induced factors.

Methods

Atmospheric Data and Processing

All atmospheric data used in this research are acquired from the NARR (Mesinger et al. 2006) data set. Two variables are used to create separate synoptic categorizations over the region of study: 1200 UTC MSLP and daily mean T850, both extracted for the domain 20°–35°N, 95°–70°W for 1979–2012. Daily mean temperature fields at the 850-mb level were selected in order to depict larger-scale thermal patterns in the lower troposphere. This level was determined to best explain the weather situations on the broader scale that lead to a cold SST event. MSLP data were selected to give an indication of wind speed, wind direction, surface water transport, and potential advection into the region.

NARR data were acquired at the full ~32-km resolution available; however, to match our previous research classifying MSLP circulation patterns (Sheridan et al. 2013), every tenth data point is sampled from the full 4,503-point data set, resulting in 450 data points across the domain being used in the classification and an average resolution of 320 km. As has been suggested elsewhere (Demuzere et al. 2009), a coarser resolution is more appropriate for regional-scale map pattern classifications when accounting for smaller-scale variability in the classification is undesirable.

The classification of 850-mb temperature into patterns is performed via unrotated S-mode principal components analysis with the correlation matrix (as described in Yarnal 1993) and the TwoStep Clustering component (SPSS Inc. 2001) in SPSS statistical software. Nine principal components with eigenvalues greater than 1 were retained for incorporation into the clustering algorithm, accounting for 98.6 % of the variance in the daily 850-mb temperature fields in the domain. While this threshold for retaining PCs is a common approach in map pattern classifications, it also demarcates the threshold at which each retained PC is accounting for at least as much variance in the data set than any single variable it is replacing (Yarnal 1993). Cluster analysis on these PCs resulted in identification of ten discrete temperature patterns (TPs); each day in the period of record is assigned to one of these TPs.

Developed initially for previous research, a very similar classification was performed to categorize each day into one of ten circulation patterns (CPs; the original classification is described in full detail in Sheridan et al. 2013). Prior to classification, the MSLP field for each day was averaged for the entire spatial domain, with this average then being subtracted from the raw value for each grid point on that day, resulting in a 'spatial anomaly' data set. These spatial anomalies were then subjected to the same two-part clustering procedure used for the classification of the temperature patterns, whereby an s-mode principal components analysis is followed by the TwoStep cluster analysis of the 12 retained PCs with eigenvalues greater than 1 (Sheridan et al. 2013). The spatial anomaly MSLP data set was chosen for the classification of CPs, as SLP gradients can be readily associated with wind properties and advection of cold air into the area. However, for temperature patterns, an absolute measure was thought to be more useful for an application to sea-surface temperatures. The ten CPs are the same as those produced in Sheridan et al. (2013); as that data set ends in 2009, the classification is extended through 2012 via creating principal component scores for the new years based on the original PCs and classifying each day into the pattern whose mean PC scores were most similar to the day's PC scores, using a sum of squared errors.

Satellite Data Processing

The satellite ocean data used in the study consist of two different product types: (1) blended microwave-infrared (MW-IR) optimally interpolated (OI) product that combines measurements of SST from the Tropical Rainfall Measuring Mission (TRMM), or TRMM Microwave Imager, Advanced Microwave Scanning Radiometer for NASAs Earth Observing System, WindSAT microwave radiometer, Moderate Resolution Imaging Spectrometer thermal infrared products at 9-km pixel resolution (2006–2013) and (2) infrared SST product from the NOAA/NASA AVHRR Ocean Pathfinder dataset at 4 km resolution (1981–2012).

Our main intent was to use reliable, consistent SST with adequate spatial and temporal resolution. The blended OI MW-IR SST product provided by Remote Sensing Systems, Inc. (RSS) offers improvements in spatial resolution when compared with single microwave sensor options and increased temporal resolution when compared with infrared products (Reynolds et al. 2007). OI is a widely used method in oceanography that makes use of irregularly spaced SST data (in time and space) to interpolate it consistently on a grid (Reynolds et al. 2007). Microwave retrievals of SST are measured through clouds and represent an advantage over the traditional thermal infrared SST observations that require a cloud-free field of view (Wentz et al. 2000). As a result, ocean areas with persistent cloud coverage were available on a daily basis providing improved temporal resolution. In situ validation of microwave SST retrievals revealed low mean bias and standard deviation errors when matched to buoy data (Gentemann et al. 2004, 2010; Reynolds et al. 2007) with overall accuracy comparable to that of infrared retrievals (Hu et al. 2009). No filtering was applied on the MW-IR SST image dataset.

AVHRR Pathfinder data include near-daily SST at 4-km spatial resolution. Pathfinder SST are consistently measured and used in applications from thermal stress detection and evaluation in coral reef systems, to climate indicator development (Halpern et al. 2008; Bruno et al. 2007; Reynolds et al. 2002; Casey and Cornillon 2001). SST estimates were obtained from and developed by the University of Miami's Rosenstiel School of Marine and Atmospheric Science and the NOAA National Oceanographic Data Center. The Pathfinder V. 5.0 Program measures SST data for both the ascending pass (daytime) and descending pass (nighttime) at 4 km resolution.

A full SST climatology was constructed for both blended MW-IR and Pathfinder datasets using all individual satellite measurements. The development of consistent near-daily time series of SST allowed for visual interpretation of SST variations and for the evaluation of spatiotemporal patterns of variability and linkages to CPs and TPs. We used standard algorithms for both Pathfinder IR and blended IR/MW images of bulk/skin temperature summarized in Kilpatrick et al. (2001) and Wentz et al. (2000), respectively. For Pathfinder SST, the Reynolds OI standard Version 2 algorithm removes pixel artifacts, null values, and exceedingly high/low pixel values prior to our analysis. All atmospheric and SST data analysis was presented for January, February, and March data only (unless otherwise noted). For each SST image used in the analysis, pixels were extracted along a transect line spanning three biogeographic sub-regions: central and southern WFS, Florida Keys, and for an area outside of St. Joseph Bay (Fig. 2).

Analytical techniques to calculate SST climatological anomaly and variability terms were based on calculations from Sheridan et al. (2013) and Pirhalla et al. (2009). SST anomaly (SSTA) was calculated as[1]

$$SSTA_{J\,yr} = \frac{SST_{J\,yr} - \overline{SST}_J}{\sigma SST_J}$$

where subscripts J and yr are Julian day and year. $SST_{J,yr}$ is the SST on Julian day J, and $\overline{SST}_J$ is the grand (long-term) mean for Julian day J of all years. To normalize for seasonal SST variability, anomalies were divided by the σSST, the climatological standard deviation for Julian day J.

We first examined climatological SST anomaly and variance estimates to assess climatological SST distribution patterns over seasonal to annual cycles, then developed an iterative calculation for SST temporal change as an observed moving CSI, investigating multiple temporal intervals (e.g., 7, 14, 21 day cycles) and lag scenarios (e.g., previous 14 and 21 days) to identify the optimal combination. For this work, the calculation of CSI uses the sum of SST difference over 14 day cycles to highlight consecutive days with the most significant SST drops, with CSI (observed) defined as

$$CSI_{t(obs)} = \left\{ \sum_{b=t-1}^{b=t-7} \sum_{a=t}^{a=t+7} (SST_a - SST_b) \right\} * 0.07$$

where CSI_t is SST cold-stress index centered at day t, variables b and a denote days before and after t, respectively. SST_a and SST_b are observed sea surface temperatures. The sum captures the duration as well as the magnitude of the difference and thus is not the same as using a single maximum difference over consecutive days. A multiplier (0.07) was applied as a scaling factor to adjust the range between 4 and −4.

Examining SST Response to Circulation and Temperature Patterns

To assess the lag–response relationship between weather and SST, relative frequencies of weather pattern conditions were assessed following similar methods from Sheridan et al. (2013). Relative frequencies of winter CPs and TPs for a given day were computed by first calculating the number of occurrences (days) of each CP and TP over the previous 21-day period, then calculating anomalous frequency by subtracting this from the mean numbers of occurrences over the same 21-day period across all calendar years in the data set.

[1] It should also be noted that SSTA, as well as the SST variables in this paper, were computed for each pixel. We have omitted subscripts that would denote location (such as x, y) to keep the formulas readable.

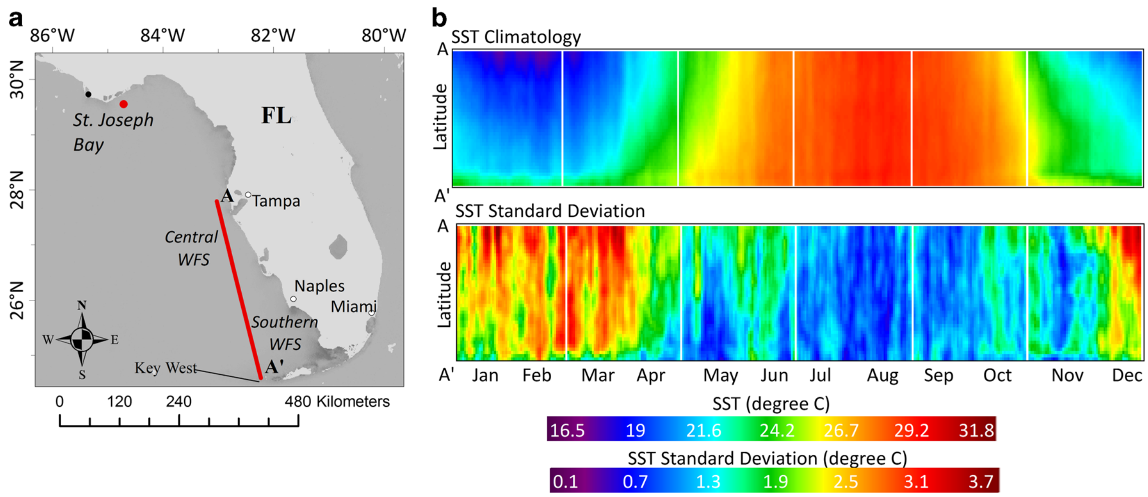

Fig. 2 Map of study region (**a**) and Hovmöller diagrams (**b**) of SST mean and standard deviation over an annual cycle, derived for 2006 to 2013. Hovmöller plots show daily running mean SST distribution (**b**, *top*) and SST variability (**b**, *bottom*) during a typical annual cycle along a north–south latitudinal transect line from approximately Tampa Bay to Key West

The relationship between CP and TP frequency and SST was assessed via correlation analysis. Significances of correlations were computed, with an effective sample size adjustment to account for the high temporal autocorrelation in the data sets (Bretherton et al. 1999):

$$N' = (N)\frac{1-r_1r_2}{1+r_1r_2}$$

where N' is the effective sample size, N is the original sample size, and r is the Pearson correlation coefficient at lag1 for each of the two variables being analyzed in each correlation analysis.

Following correlation analysis, CPs and TPs were isolated, and then grouped as aggregates that exhibited the most significant correlation with absolute SST and derived SST deviation over seasonal to annual cycles. As shown below, one circulation pattern, Atlantic Low (CP3), and one thermal pattern, Cold Air Outbreak (TP4), show the strongest correlation with extreme SST events. To explore their influence further, a circulation–temperature pattern aggregate (CTPA) combining CP3 and TP4 was calculated as the product of the total number of occurrences of these patterns relative to the previous 21-day period, then binned by month. Next, we developed cold- stress likelihood scenarios based on weather pattern frequency bins. Composited MW/IR SST scenario maps were calculated for all pixels in the study area using similar procedures to those in Sheridan et al. (2013), as the sum of the 3-day mean SSTA divided by the number of days that fell into each frequency bin, for each weather pattern (wp) analyzed:

$$\mathrm{Deviation}_{J,\,WP} = \frac{\overline{\sum_J^{t-20}\mathrm{SSTA}}}{n\,(wp)} - 1$$

Deviations that were statistically significant from zero ($p<0.05$ using Student's t test with two tails) were also recorded in the resultant maps.

Estimating SST and CSI from Weather Patterns

Following correlation analysis and evaluation of lag–response relationships between modeled weather patterns and observed SST values, we then estimated SST and CSI during cold-snap weather periods based on the frequency of TP4 and CP3 with emphasis on negative SST deviation from climatological mean conditions. We attribute high-frequency drops in SST to a predominant air–sea cooling effect. We then used CTPA frequency to estimate SST ($\mathrm{SST}_{(est)}$) as defined to include only those days when TP4 occurrences over the previous 21-day period were greater than or equal to 4 (about 20 % frequency) and CP3 occurrences were greater than or equal to 2 (about 10 % frequency). This was performed to highlight periods in which low temperature and circulation patterns persisted over the entire region. We estimated $\mathrm{SST}_{a(est)}$ during cold- snap based on the frequency of TP4 and CP3, as

$$\mathrm{SST}_{a(est)} = \overline{SST}_J + \left(\exp\left\{\frac{-1\sum_{b=t}^{b=t-20} tp4 * \sum_{b=t}^{b=t-20} cp3}{25}\right\} - 1\right) * 2.56 * \sigma\overline{SST}_J$$

where $\overline{SST}_J$ is the climatological SST mean and $\sigma\overline{SST}_J$ is the climatological SST standard deviation on Julian day J.

The terms $\sum_{b=t}^{b=t-20} tp4$ and $\sum_{b=t}^{b=t-20} cp3$ are the sum of occurrences of weather patterns TP4 and CP3 over the previous 21 days from time t. Coefficients of 25 and 2.56 are scaling constants.

Finally, utilizing observed and estimated SST values, we then estimate CSI_t as:

$$\mathrm{CSI}_{t\ (\mathrm{est})} = \left\{ \sum_{b=t-1}^{b=t-7} \sum_{a=t}^{a=t+7} \left(\mathrm{SST}_{\mathrm{a(est)}} - \mathrm{SST}_b \right) \right\} * 0.07.$$

The variable $\mathrm{CSI}_{t(\mathrm{est})}$ is estimated at time t for each MW-IR SST pixel, utilizing $\mathrm{SST}_{a(\mathrm{est})}$ out to 7 days.

Results

Seasonal Patterns of SST Variability

The seasonal cycle of SST across the study region is depicted in Fig. 2. The mean SST seasonal cycle (b; top) reveals summer maximums near 30 °C throughout the transect; during the winter, apart from a broad cooling, a sharp latitudinal gradient appears, separating colder nearshore waters to the north from warmer waters to the south, due mainly to influences from the Florida Current. During winter, temperatures thus range from 16 °C in northern areas to approximately 25 °C near Key West. Temporal patterns of SST reveal stronger variability during winter and early spring and a greater variability farther north (b; bottom), likely associated with more frequent cold front passages, storm systems, shifts in alongshore seasonal surface currents, and Ekman-induced (wind-stressed forced) transport.

CP and TP Descriptions

The ten CPs used in this research from Sheridan et al. (2013) can be found in Fig. 3. Figure 4a displays the mean 850-mb temperature across all days categorized into each of the ten TPs classified in this research, along with the seasonality of each of these patterns. Due to increased synoptic-scale weather variability in the winter season, the majority of TPs exhibit a non-summer peak; however, the summer-dominant patterns (TP9 and TP10) are the most frequent. While TP1 and TP8 also show abnormally cold air advecting into the GOM region in the winter season, TP4 represents the coldest weather specifically across the region of interest (Florida Coasts), likely due to the passage of a strong cold front. Figure 4b highlights the anomalously cold 850-mb temperatures that accompany TP4 even within the extended cold season of interest (December–March). As the broad area of cold lower tropospheric temperatures in TP4 (hereafter also termed 'cold air outbreak') is likely associated with cold surface temperatures, among all T850 patterns it is the main pattern assessed in the remainder of this research.

SST and Circulation–Temperature Pattern Associations

To assess measures of association between weather and water properties, Pearson correlation coefficients and measures of significance of multiple TP4, CP3, and SST response combinations for the regions of interest (December–March) are shown in Table 1. Using correlates of winter time pattern frequency as inputs, coefficients, and p values for both Pathfinder and MW-IR SST and SSTA, values were significant for CP3 and TP4 ($r<-0.39$ to -0.65). CP3 exhibits the most favorable circulation related to cold air outbreaks, drops in 850 temperatures, and low daily SST, while the other nine CPs tested revealed minimal association and few significant results (not shown). The cold air outbreak pattern (TP4) shows a significant negative correlation with all measures of SST and severe cold-water events (i.e., increased frequency of TP4 is significantly associated with decreased SST). Significance tests also reveal that, in most cases, CP3, TP4, and CTPA frequencies have slightly stronger correlations to SST and SSTA than do daily air temperature minimums, compiled for Key West and Miami meteorological stations (from Karsten Shein; NCDC), especially for the MW-IR-based measurements. TP4 frequency shows marginally higher correlation than CP3 frequency when compared with the SST and SSTA.

Weather Pattern Frequency Relationships with SST

Time series of previous 21-day CP and TP relative frequencies (bars) and daily-scale normalized SST anomaly and CSI values (lines) are displayed in Fig. 5. Plots reveal heightened periods of anomalous frequencies coincident with anomalously negative SST and CSI along the north–south transect. Heightened periods of CP3 (5a), indicative of Atlantic Low development are shown in positive deviations, especially during winter 2010/11, and coincident with heightened TP4 (5b), indicative of cold-snaps. Also shown are the peaks during 2010/2011 when frequency counts of CP3 and TP4 were aggregated as a product term (CTPA; 5c). Also apparent is the strong and abrupt CSI response during winter months of the same years (5b), where plummeting index values were followed by immediate increases on weekly scales. The CSI shows a sharp negative deviation during the first 2-week period in January of 2010 and December–January of 2010/2011. Climatological SST anomaly shows a prolonged negative response for the months of January through April, 2010, and December 2010 through March of 2011. A less

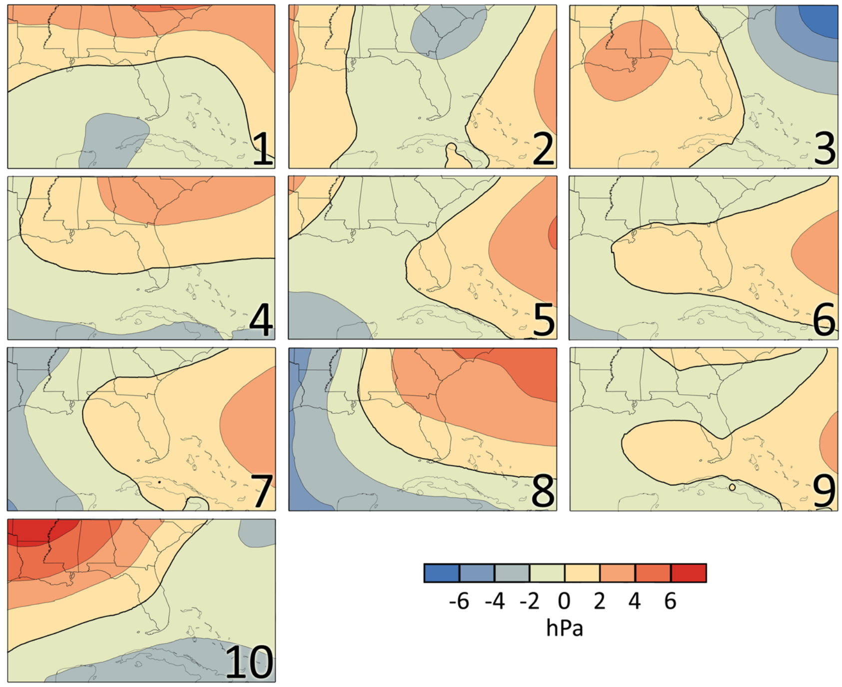

Fig. 3 Mean sea-level pressure anomalies associated with each of the ten CPs. Figure from Sheridan et al. (2013); copyright American Meteorological Society

pronounced cold-snap event occurred along the Gulf-side in winter of 2009 with more widespread impacts on the Atlantic-side (not shown).

Composite maps of SSTA distribution by CP3 and TP4 frequency bins are shown for January–March (Fig. 6). This figure shows the spatial distribution of the SST-to-CP/TP relationship quantified in Table 1, indicating that SSTs are well below average over a large portion of the study domain with increasing frequency of CP3 and TP4. SST deviations for warmer patterns reveal the opposite relationship to colder patterns (not shown), i.e., increased frequency leads to higher than expected SST.

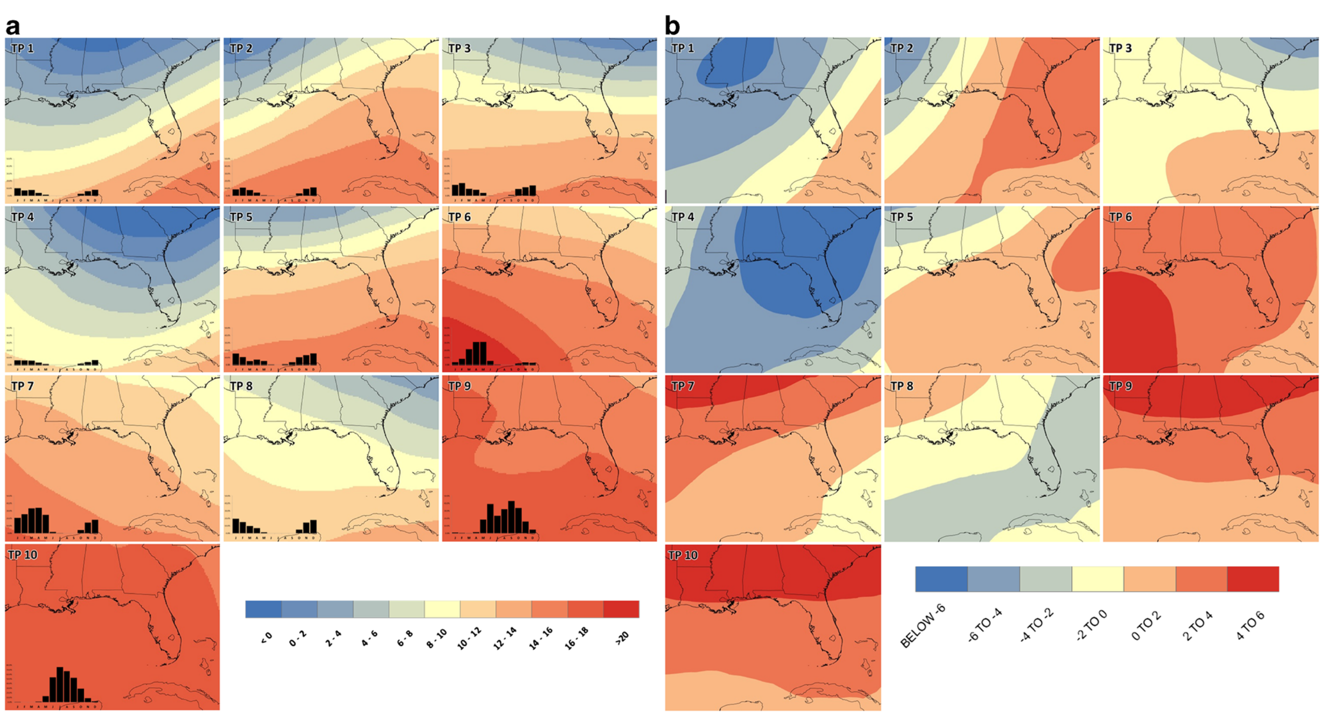

Fig. 4 Mean 850-mb temperatures (degrees Celsius) and average monthly frequency (from January (*left*) to December (*right*); bar graph in *lower left* of each map) associated with each of the ten temperature patterns (**a**) and the 850 t anomaly for each pattern in the December–March window of analysis (**b**)

Table 1 Pearson-product correlates and coefficients comparing weather pattern frequency, in situ daily temperature minimums (Tmin), Pathfinder SST (1981–2012), MW-SST (2006–2013), and SST derivatives

Pearson correlation	SST (Pathfinder)	SST anomaly (Pathfinder)	SST (MW-IR)	SST anomaly (MW-IR)
TP4 frequency	−0.438*	−0.445*	−0.541*	−0.634*
CP3 frequency	−0.394*	−0.416*	−0.527*	−0.651*
CP3 and TP4 aggregate frequency (CTPA)	−0.470*	−0.489*	−0.584*	−0.706*
Key West Tmin	0.479*	0.477*	0.422*	0.450*
Miami Tmin	0.414*	0.416*	0.367*	0.377*

Pattern frequencies were calculated as total counts of daily pattern occurrence over the previous 21 days in the time series

*$p<0.05$ level of significance

Further analysis of SST versus weather pattern frequency counts reveals a fairly consistent frequency–response relationship (Table 2). During heightened periods of CP3 and TP4 frequency, SST is consistently lower (at or below 17 °C). During periods when CP3 and TP4 frequency drops to zero, SST is near climatological normal conditions (20 °C).

CSI Coincidence with Turtle Strandings

From January 2–11, 2010, decreases of near 12 °C for air temperatures and 6 °C for water temperatures were evident in nearshore waters of the upper, middle, and lower Keys areas and the Apalachicola Bay area along the Florida Panhandle coast (Lirman et al. 2011; Roberts et al. 2014). In terms of absolute SST at time of the event, minimum observed SST along the WFS and seaward of Apalachicola Bay reached approximately 15 °C and 13 °C, respectively. Documented thermal limits for hypothermia in green turtles range from 10–15 °C, with mortality likely at 5 °C (Foley et al. 2012). In the case of 2010, biological impacts from the event were immediate with turtle hypothermic cases occurring January 7–14, with peak numbers of turtles (444) stunned on January 11. A total of approximately 1,500 turtles were found in St. Joseph Bay during the event.

The 2010 event resulted in four times the number of strandings than for the other events recorded. Plots showing combinations of observed CSI and turtle strandings in St. Joseph Bay are presented for three separate cold-snap events in 2008, 2010, and 2011–2012 (Fig. 7). Note negative CSI coincident with turtle strandings, especially in the 2010 event (Fig. 7b). Additional events to 2010 include: January 2008 (Fig. 7a), a mass Florida-wide event in February 2009 (not shown), and a smaller event in December–January 2010/2011 (Fig. 7c).

Predicted CSI from Weather Variable Combinations

Using the weather variable CTPA model to estimate CSI, the linear regression between observed and estimated CSI is shown in Fig. 8. Threshold criteria chosen for the model represent total days when TP4 were greater than 4, and CP3 were greater than 2 in the previous 21 days. Cold-stun events are labeled to highlight when estimated CSI is less than −2, the likelihood of cold-snap events and turtle stuns increases. Note that, during the peak of the 2010 event, observed and estimated CSI were strongly negative (near −4) and coincident with peaks in turtle strandings.

Discussion

Atmospheric Pattern–SST Relationships

Several studies have documented major processes that influence SST variability in South Florida and GOM coastal ecosystems, especially variability surrounding the cold-water event of January 2010 (Wiseman and Sturges 1999; Liu and Weisberg 2007; Lirman et al. 2011; Gramer 2013). Gramer (2013) established that variability surrounding extreme anomalously cold events is strongly dependent on air–sea cooling, especially for areas with the shallowest and flattest topography, and consequently in close proximity to natural resources and habitats. This emphasizes the importance of understanding synoptic variations in how SST may become lethal for marine species, especially in areas where entire populations may be most susceptible.

Climatological analysis of SST reveals that the 2010 cold-air and water event was the most significant on record in terms of regional SST deviation and also for event duration. A period of strong negative SSTA persisted over 3 months post-event, from January through March, 2010. The event was also marked by the most significant drops in SST over a 14-day duration, as evidenced by CSI time series (Fig. 7).

The overall weather-related factors and mechanisms associated with cold-snap events and impacts are depicted well using synoptic climatological methods. In particular, CP3 and TP4 are winter-dominant and highly coincident with extreme cold and mortality. The co-occurrence of these patterns and increased frequency during cold water events likely influence SST in combination, whereby cold-core high pressure to the west, centered on average near Louisiana, coupled with

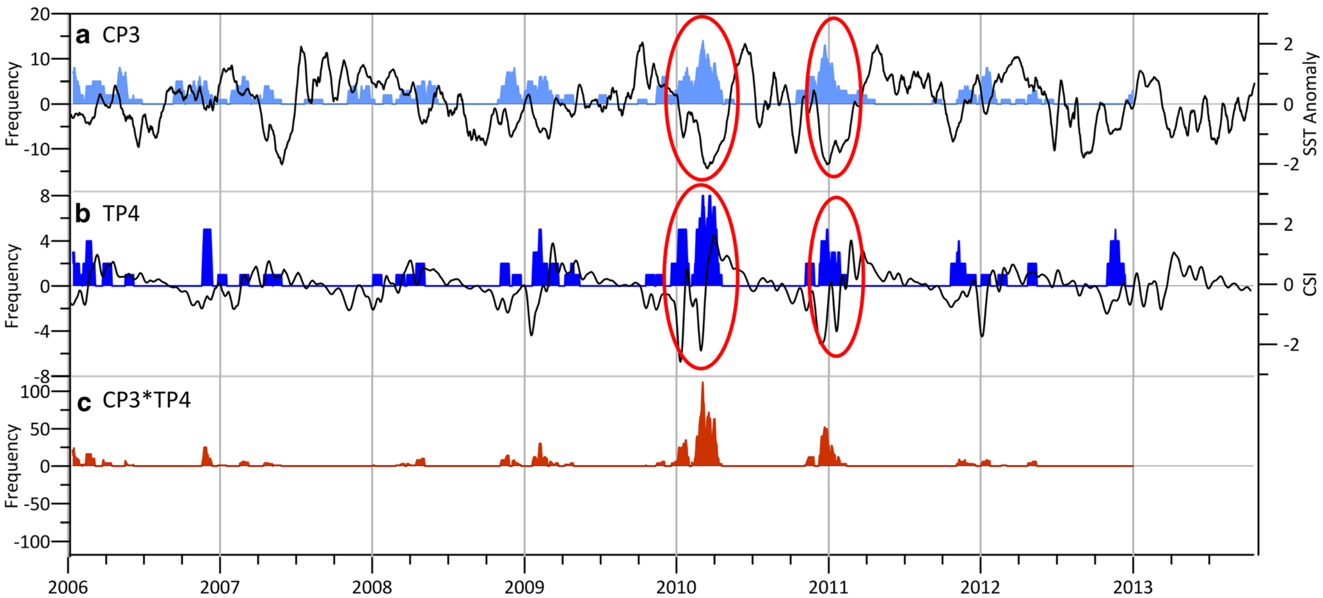

Fig. 5 Time series of observed of circulation and temperature pattern frequency anomalies, SST anomaly and SST moving index (CSI) values for all days in the time series (2006–2013). The strong cold-snap events of January 2010 and December 2011 are noted (*ellipses*)

Atlantic Low development, may support a stronger than normal east-to-west surface pressure gradient and strong north-to-south wind fields, inducing a more southward protrusion of cold Arctic air, and thus, prolonged abnormally cold temperatures as manifest in the TP4 pattern. The co-varying nature of these two patterns implies that increased Atlantic cyclone development may have significant influence on southward intrusions of colder than normal temperatures and on future cold extremes throughout Florida.

Composites of anomalous SST by CP3 and TP4 relative frequencies show a reliable frequency–response pattern of weather conditions favorable for producing cold-snap events. The higher the combined frequencies, the more significant drops in SST exhibited. Other prevailing wintertime circulation patterns reveal a moderate to weak association with decreased air temperatures and SST. As evidenced by CP3 and TP4 co-occurrence and elevated frequencies during significant SST drops and cold-stress events, CP3 and TP4 are

Fig. 6 Mean sea surface temperature anomaly (SSTA) by frequency bins of CP3, TP4 (*top two rows*) and CP3*CP4 (*bottom row*) for January, February, and March. SSTA was calculated as the 3-day mean SST minus expected SST for that location and Julian day, normalized by expected standard deviation of SST for dates that matched the following frequency (counts): CP3, TP4 (*top two rows*): 0, 1–2, 3–5, >5; CP3*TP4 (*bottom row*): 0, 1–5, 6–12, >12. The figure enables visualization of positive (*red*) and negative (*blue*) SSTA response associated with increased (decreased) frequency range, respectively

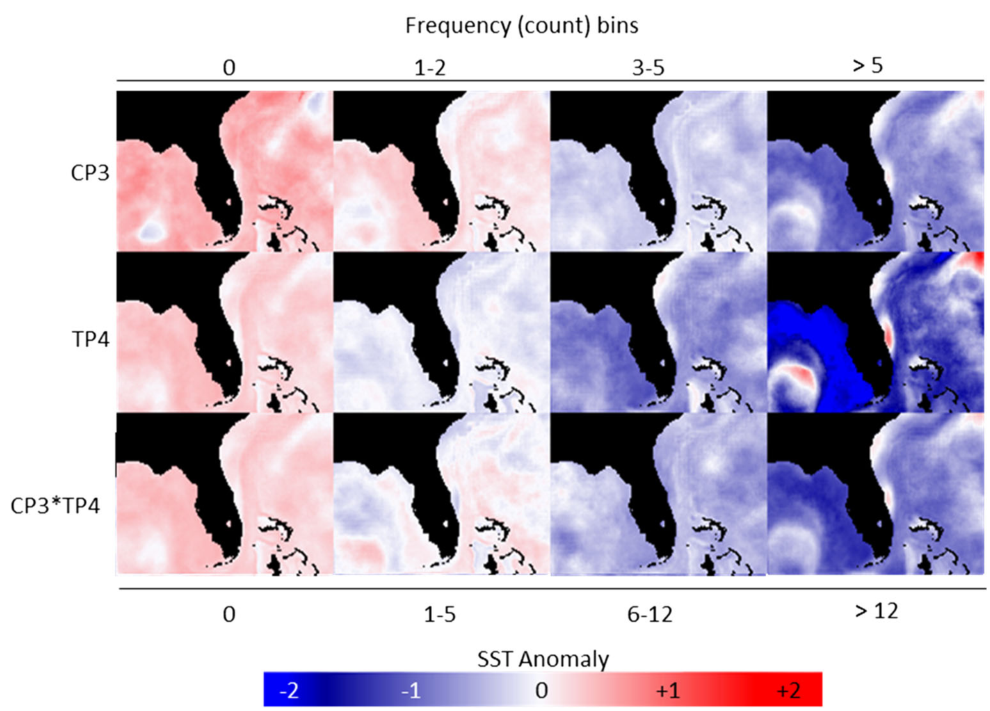

Table 2 Average winter (Jan–Mar) MW-SST (degrees Celsius) by frequency counts of CP3 (columns) and TP4 (rows) in the previous 21 days

	CP3												
	Pattern Frequeny	0	1	2	3	4	5	6	7	8	9	10	11
TP4	0	23.7	20.4	19.2	18.2	18.2	17.2	17.6	16.4	15.9			
	1	24.6	17.3	20.1	19.5	19.3	16.9	17.8	16.6				
	2	23.3	22.4		15.7	13.8	14.1		14.4	14.6	13.2		
	3	22.1				14.8						15.6	
	4	20.8		17.1		16.1	16.3	15.9	15.7	14			
	>5							15.9					14

SST were extracted and averaged for pixels near Apalachicola Bay, FL. SST below 16 °C (blue), 20 °C (orange), and 24 °C (red). SST less than 16 °C (blue) are associated with CP3 greater than 5, or TP4 greater than 1

likely reliable indicators to track and monitor lethal SST at or below thermal limits for species. In terms of duration of weather patterns, prolonged frequency of TP4, especially when paired with CP3 frequency, appears to be an important indicator for cold-snaps. TP4 or CP3 counts shorter in duration seem less likely to induce cold snaps.

Turtle Stuns and the Cold-Stress Index

The SST moving cold-stress index, or CSI, showed a more distinct drop and rise after the cold air outbreak, and when paired with turtle strandings data, showed strong coincidence with acute responses in turtle hypothermic cases. This would indicate that the CSI, which emphasizes the duration and magnitude of SST decreases over consecutive days, may be an important qualifier in understanding the relationship among air–sea cooling, biological response, and impacts. As such, a regionally derived CSI may exploit an effective means for tracking and monitoring in-water temperature indicators near lethal limits for species.

The temporal patterns of negative CSI and increased numbers of turtles that were stunned reveal that most turtle strandings recorded were during mid-phase of low CSI (Fig. 7). In the two succeeding months after the cold stun

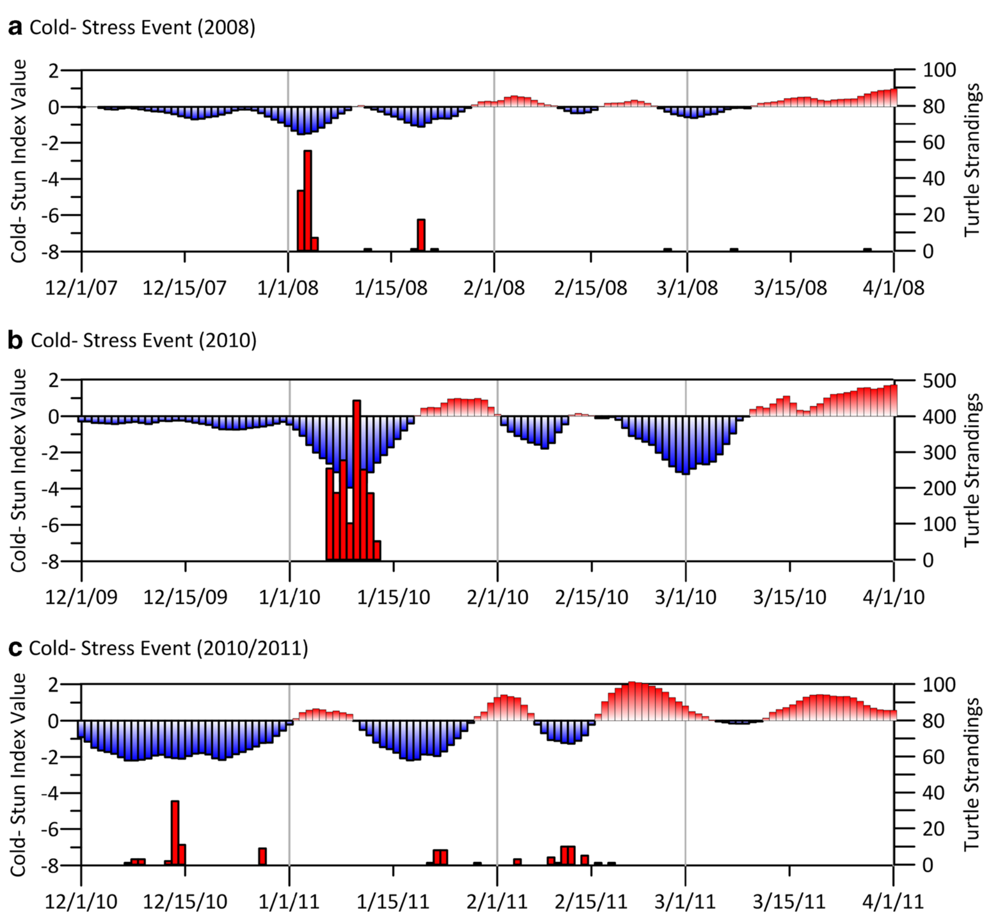

Fig. 7 Relationships of observed cold-stress index (CSI) values calculated for Tampa, FL, and turtle strandings data, compiled for St. Joe's Bay, near Apalachicola, FL. Note that stranding scales are not the same

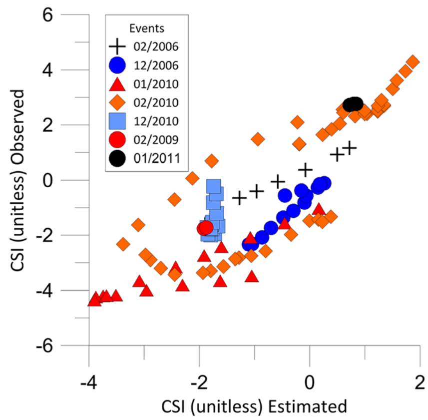

Fig. 8 Regression plots of observed versus estimated CSI values for selected cold events calculated for the northern part of Tampa, FL, region

event of January, 2010, there was another episode of negative CSI and SSTA, with no turtle stuns recorded. This is speculated to be a function of the severity of the initial event, whereby either turtles migrated out of the area after the event, or too few remain after being collected (Roberts, pers. comm.).

Synoptic Modeling Implications and Limitations

The parameterizations used to estimate SST and CSI during cold air outbreaks were formulated using weather pattern frequency levels over the previous 21 days to simulate the high-frequency drivers and complex air–sea cooling processes during cold-snap events. This was accomplished to emphasize the temporal intervals associated with maximum negative SST response. Using thresholds of TP4 counts greater than 4 and CP3 counts greater than or equal to 2, the model captured seven unique events. Model tendency was to over-predict CSI using low threshold counts (<2) for both CP3 and TP4 and over-predict when TP4 frequencies were high and CP3 frequencies were alternatively low.

The frequency threshold levels and parameterizations for the model were based on the premise that CP3 cumulative frequency acts to reinforce cold-air intrusion over the Florida region, and as such, increases the likelihood and persistence of the cold air outbreak pattern (TP4). Thus, the model relies on higher CP3 frequency levels to reinforce the cold air and the dramatic decreases in surface water temperatures.

Although weather does act as a trigger to initiate cold air and water response, there are numerous provisions to the use of a cold-stress index and weather-induced cold-stress model. For instance, ocean transport may be a more significant influence on anomalously cold SST than weather pattern frequencies alone. Liu and Weisburg (2007) surmised that oceanic circulation along the inner shelf areas may be dominated by cooler waters injected southward, perhaps mixing with colder bottom water during Ekman-induced upwelling events. Since upwelling in the region has been attributed to the passage of synoptic cold fronts and to proximity and location of tropical storms (e.g., trailing side of storms), we speculate that air–sea cooling can work in combination with southward transport *and* upwelling-related processes to influence SST to near-critical limits for species.

In addition, anomalously negative SST can remain far below mean winter conditions for extended periods as shown in the SSTA time series (Fig. 5). Thus, ambient waters may be affected by weather variations but with less dramatic drops in SST, and thus, less consequence on species.

Summary and Conclusions

This study considers whether atmospheric patterns derived using synoptic climatological methods may provide insight into key ecological thresholds in systems. In this paper, we defined characteristics of SST as a lethal response indicator, whereby persistence of specific weather patterns can act to reinforce a negative behavioral or physiological response on habitats, species, and populations. Synoptic weather patterns appear to be temporally linked to cold-snap frequency, duration, and magnitude of events along the entire study area. Specific temperature and circulation patterns (TP4, CP3) have a significant correlation with drops in sea surface temperature and to thermal threshold tolerances associated with the 2010 event.

In the context of global change and variability, understanding weather factors and drivers surrounding cold air outbreaks will allow for improved predictions of likelihood of these outbreaks and future impacts. The current study provides new insights and novel approaches that may form the basis of a useful tool in marine ecology and conservation. For example, a weather-driven CSI introduced here represents an empirical link between air–ocean ecosystem driver–response relationships from state-of-the-art weather model statistics and temporally robust, reliable satellite SST data. Since blended satellite SST data provide refined daily-scale temporal resolution, we believe the use of MW-IR SST (even at a coarser spatial resolution than high resolution IR-SST) has a strong potential to monitor and track cold-stress events for the region. In addition, MW-IR SST observations along shelf environments can be extracted and applied in broader biogeographic marine contexts.

A prior knowledge of cold air outbreaks and early warning of potentially lethal SSTs would support a multitude of coastal surveillance and adaptive management response functions which may include: improved management response for restoration and protection of impacted populations, improved marine resource and habitat impact evaluations, and ultimately improved preparedness for management of all aquatic and terrestrial systems impacted by regional climate variability and changes.

Identified as part of this study were cold-stress events (i.e., specific stress-related events where species undergo metabolic, physiological, or behavioral changes resulting in an ecological impact). Specific lethal threshold temperatures vary for individual species and marine ecosystems. Although individual limits for species were not identified or sought in this paper, the mechanisms that underlie the events were identified. Inland bays, marshes, and coral reef systems respond much faster to air temperature changes than deeper shelf systems, and depend highly on bathymetry and topography of the affected area. However, understanding the scales over which weather patterns and events will affect SST and species will allow researchers and coastal resource managers to identify potentially lethal events and evaluate their impact on individual species and/or multiple resources.

The linkages between atmospheric variability, ocean and ecosystem structure and function are still not fully understood, nor are how these linkages and processes vary over space and time. With the current observational and ecological modeling tools available, researchers have only begun to understand the impact of climate and weather variations on physical and chemical changes and influences on ecological thresholds. However, from this effort, clear patterns have emerged linking the air–sea cooling phenomena to both satellite observational and biological response and impact. Further research is needed to first characterize the likelihood of significant threshold patterns and events, and predict or forecast the response in terms of a biological threshold and subsequent management response. This is particularly relevant to living marine resources for sustainable ecosystem services and management response.

Acknowledgments We thank the personnel at the Remote Sensing Systems, Inc., data processing group, for making the blended microwave-infrared SST products available; NOAAs National Oceanographic Data Center Satellite Oceanography Team for providing consistent Pathfinder SST data products; and NOAAs Earth System Research Laboratory, Physical Sciences Division, for providing up-to-date gridded NCEP North American Regional Reanalysis products. We thank Karsten Shein of the National Climatic Data Center for providing up-to-date in situ climatological data for multiple South Florida stations. We acknowledge and appreciate the input of Kelsey Roberts of the University of South Florida during manuscript development. Funding support for the study was provided by NOAA's National Center for Coastal Ocean Science. Last of all, we would like to pay kind tribute and dedication to Doug Pirhalla's father, Joseph William Pirhalla, who passed away on November 3, 2013, for providing Doug with strength and inspiration during the entire writing process, and throughout life. His hugs and kind-hearted words are within his loved ones hearts, now and forever.

References

Avens, L., C. Harms, E. Anderson, L. Goshe, A. Goodman, W. Cluse, M. Godfrey, J. Braun-McNeill, and B. Stacy. 2012. 448 Turtles in the freezer: and population assessment of green sea turtles stranded dead in St. Joseph Bay, Florida, USA, during the January 2010 mass cold-stunning. Proceedings of the thirty-first annual symposium on sea turtle biology and conservation, NOAA Technical Memorandum NMFS-SEFSC-631.

Barlas, M.E., C.J. Deutsch, M. Witt, and L.I. Ward-Geiger. 2011. Florida manatee cold-related unusual mortality event, January–April 2010. Final report to USFWS (grant 40181AG037). Florida Fish and Wildlife Conservation Commission, St. Petersburg, FL.

Bretherton, C.S., M. Widmann, V.P. Dymnikov, J.M. Wallace, and I. BladéI. 1999. The effective number of spatial degrees of freedom in a time-varying field. *Journal of Climate* 12: 1990–2009.

Bruno, J.F., E.R. Selig, K.S. Casey, C.A. Page, B.L. Willis, C.D. Harvell, H. Sweatman, and A.M. Melendy. 2007. Thermal stress and coral cover as drivers of coral disease outbreaks. *PLoS Biology* 5(6): e124. doi:10.1371/journal.pbio.0050124.

Carpenter, K.E., M. Abrar, G. Aeby, R.B. Aronson, S. Banks, A. Bruckner, A. Chiriboga, J. Cortes, J.C. Delbeek, L. DeVantier, G.J. Edgar, A.J. Edwards, D. Fenner, H.M. Guzman, B.W. Hoeksema, G. Hodgson, O. Johan, W.Y. Licuanan, S.R. Livingstone, E.R. Lovell, J.A. Moore, D.O. Obura, D. Ochavillo, B.A. Polidoro, W.F. Precht, M.C. Quibilan, C. Reboton, Z.T. Richards, A.D. Rogers, J. Sanciangco, A. Sheppard, C. Sheppard, J. Smith, S. Stuart, E. Turak, J.E.N. Veron, C. Wallace, E. Weil, and E. Wood. 2008. One-third of reef-building corals face elevated extinction risk from climate change and local impacts. *Science* 321(5888): 560–563.

Casey, K.S., and P. Cornillon. 2001. Global and regional sea surface temperature trends. *Journal of Geophysical Research* 14(18): 3801–3818.

Colella, M.A., R.R. Ruzicka, J.A. Kidney, J.M. Morrison, and V.B. Brinkhuis. 2012. Cold-water event of January 2010 results in catastrophic benthic mortality on patch reefs in the Florida Keys. *Coral Reefs* 10: 1–12.

Demuzere, M., M. Werner, N.P.M. van Lipzig, and E. Roeckner. 2009. An analysis of present and future ECHAM5 pressure fields using a classification of circulation patterns. *International Journal of Climatology* 29(12): 1796–1810.

Foley, A.M., D. Bagley, R. Bailey, L. Belskis, B. Brost, N. Evou, R. Hardy, S. Hirama, A. Hoffman, M. Koperski, A. Meylan, K. Minch, L. Patrick, J. Provancha, S. Schaf, B. Schroeder, B. Stacy, W. Teas, R. Trindeli, and B. Witherington. 2012. Report on a massive hypothermic stunning event of sea turtles in Florida during January 2010. Proceedings of the thirty-first annual symposium on sea turtle biology and conservation, NOAA Technical Memorandum NMFS-SEFSC-631.

Francis, J.A., and S.J. Vavrus. 2012. Evidence linking Arctic amplification to extreme weather in mid-latitudes. *Geophysical Research Letters* 39, L06801. doi:10.1029/2012GL051000.

Fry, F.E.J. 1971. The effect of environmental factors on the physiology of fish. In *Fish physiology*, ed. W.S. Hoar and D.J. Randall, 1–98. New York: Academic Press.

Gentemann, C.L., F.J. Wentz, C.A. Mears, and D.K. Smith. 2004. In situ validation of Tropical Rainfall Measuring Mission microwave sea surface temperatures. *Journal of Geophysical Research* 109, C04021. doi:10.1029/2003JC002092.

Gentemann, C.L., T. Meissner, and F.J. Wentz. 2010. Accuracy of satellite sea surface temperatures at 7 and 11 GHz. *IEEE Transactions on Geoscience and Remote Sensing* 48: 1009–1018.

Gramer, L. J. 2013. Dynamics of sea temperature variability on Florida's reef tract. Open Access Dissertations. Paper 1083.

Halpern, B.S., S. Walbridge, K.A. Selkoe, C.V. Kappel, F. Micheli, C. D'Agrosa, J.F. Bruno, K.S. Casey, C. Ebert, H.E. Fox, R. Fujita, D. Heinemann, H.S. Lenihan, E.M.P. Madin, M.T. Perry, E.R. Selig, M. Spalding, R. Steneck, and R. Watson. 2008. A global map of human impact on marine ecosystems. *Science* 319(5865): 948–952. doi:10.1126/science.1149345.

Hare, J.A., M.J. Wuenschel, and M.E. Kimball. 2012. Projecting range limits with coupled thermal tolerance—climate change models: an example based on gray snapper (*Lutjanus griseus*) along the U.S. East Coast. *PLoS ONE* 7(12): e52294. doi:10.1371/journal.pone.0052294.

Hu, C., F.E. Muller-Karger, B. Murch, D. Myhre, J. Taylor, R. Luerssen, C. Moses, C. Zhang, L. Gramer, and J. Hendee. 2009. Building an automated integrated observing system to detect sea surface temperature anomaly events in the Florida Keys. IEEE Trans. *Geoscience and Remote Sensing* 47: 1607–1620.

Hughes, T.P., A.H. Baird, D.R. Bellwood, M. Card, S.R. Connolly, C. Folke, R. Grosberg, O. Hoegh-Guldberg, J.B.C. Jackson, J. Kleypas, J.M. Lough, P. Marshall, M. Nyström, S.R. Palumbi, J.M. Pandolfi, B. Rosen, and J. Roughgarden. 2003. Climate change, human impacts, and the resilience of coral reefs. *Science* 301(5635): 929–933. doi:10.1126/science.1085046.

Huth, R., C. Beck, A. Philipp, M. Demuzere, Z. Ustrnul, M. Cahynová, J. Kysely, and O.E. Tveito. 2008. Classifications of atmospheric circulation patterns. *Annals of the New York Academy of Sciences* 1146(1): 105–152.

Joyce, T.M. 2002. One hundred plus years of wintertime climate variability in the eastern United States. *Journal of Climate* 15: 1076–1086.

Kilpatrick, K.A., G.P. Podestfi, and R. Evans. 2001. Overview of the NOAA/NASA advanced very high resolution radiometer Pathfinder algorithm for sea surface temperature and associated matchup database. *Journal of Geophysical Research* 106: 9179–9197.

Kimmel, D.G., W.D. Miller, L.W. Harding, E.D. Houde, and M.R. Roman. 2009. Estuarine ecosystem response captured using a synoptic climatology. *Estuaries and Coasts* 32: 403–409.

Lirman, D., S. Schopmeyer, D. Manzello, L.J. Gramer, W.F. Precht, F. Muller-Karger, K. Banks, B. Barnes, E. Bartels, A. Bourque, J. Byrne, S. Donahue, J. Duquesnel, L. Fisher, D. Gilliam, J. Hendee, M. Johnson, K. Maxwell, E. McDevitt, J. Monty, D. Rueda, R. Ruzicka, and S. Thanner. 2011. Severe 2010 cold-water event caused unprecedented mortality to corals of the Florida Reef tract and reversed previous survivorship patterns. *PLoS ONE* 6: e23047.

Liu, Y., and R.H. Weisberg. 2007. Ocean currents and sea surface heights estimated across the west Florida shelf. *Journal of Physical Oceanography* 37: 1697–1713.

Manzello, D.P., R. Berkelmans, and J.C. Hendee. 2007. Coral bleaching indices and thresholds for the Florida Reef tract, Bahamas, and St. Croix, US Virgin Islands. *Marine Pollution Bulletin* 54: 1923–1931.

Mesinger, F., G. DiMego, E. Kalnay, K. Mitchell, P.C. Shafran, W. Ebisuzaki, D. Jovic, J. Woollen, E. Rogers, E.H. Berbery, M.B. Ek, Y. Fan, R. Grumbine, W. Higgins, H. Li, Y. Lin, G. Manikin, D. Parrish, and W. Shi. 2006. North American regional reanalysis. *Bulletin of the American Meteorological Society* 87: 343–360.

Monaldo, F., T. Sikora, S. Babin, and R. Sterner. 1997. Satellite imagery of sea surface temperature cooling in the wake of 1996 Hurricane Edouard. *Monthly Weather Review* 125(10): 2716–2721.

Morey, S.L., M.A. Bourassa, D.S. Dukhovskoy, and J.J. O'Brien. 2006. Modeling studies of the upper ocean response to a tropical cyclone. *Ocean Dynamics*. doi:10.1007/s10236-006-0085-y.

Pirhalla, D., V. Ransibrahmanakul, and R. Clark. 2009: An oceanographic characterization of the Olympic Coast National Marine Sanctuary and Pacific Northwest: interpretive summary of ocean climate and regional processes through satellite remote sensing. NOAA Tech. Memo. NOS NCCOS 90, 69 pp.

Pörtner, H.O. 2002. Climate variations and the physiological basis of temperature dependent biogeography: systemic to molecular hierarchy of thermal tolerance in animals. *Comparative Biochemistry and Physiology-Part A: Molecular & Integrative Physiology* 132: 739–761.

Reynolds, R.W., N.A. Rayner, T.M. Smith, D.C. Stokes, and W. Wang. 2002. An improved *in situ* and satellite SST analysis for climate. *Journal of Climate* 15: 1609–1625.

Reynolds, R.W., T.M. Smith, C. Liu, D.B. Chelton, K.S. Casey, and M.G. Schlax. 2007. Daily high-resolution-blended analyses for sea surface temperature. *Journal of Climate* 20: 5473–5496.

Roberts, K., J.M. Collins, C. Paxton, R. Hardy, and J. Downs. 2014. Weather patterns associated with green turtle hypothermic stunning events in St. Joseph Bay and Mosquito Lagoon, FL. *Physical Geography* 35: 2.

Sheridan, S.C., and L.S. Kalkstein. 2004. Progress in heat watch-warning system technology. *Bulletin of the American Meteorological Society* 85: 1931–1941.

Sheridan, S.C., C.C. Lee, M.J. Allen, and L.S. Kalkstein. 2012. Future heat vulnerability in California part I: projecting future weather types and heat events. *Climatic Change* 115: 291–309.

Sheridan, S.C., D.E. Pirhalla, C.C. Lee, and V. Ransibrahmanakul. 2013. Evaluating linkages of weather patterns and water quality responses in South Florida using a synoptic climatological approach. *Journal of Applied Meteorology and Climatology* 52(2): 425–438. doi:10.1175/JAMC-D-12-0126.1.

SPSS Inc. 2001. *The SPSS two-step cluster component: a scalable component to segment your customers more effectively*. Illinois: White paper, technical report, SPSS: Chicago.

Stenseth, N.C., G. Ottersen, J.W. Hurrell, A. Mysterud, M. Lima, K.S. Chan, N.G. Yoccoz, and B. Adlandsvik. 2003. Studying climate effects on ecology through the use of climate indices: the North Atlantic Oscillation, El Nino Southern Oscillation and beyond. *Proceedings of the Royal Society London B* 270: 2087–2096.

Weisberg, R.H., R. He, G. Kirkpatrick, F. Muller-Karger, and J.J. Walsh. 2004. A West Florida Shelf study: coastal ocean circulation influences on remotely sensed optical properties. *Oceanography* 17: 68–75.

Wentz, F.J., C.L. Gentemann, D.K. Smith, and D.B. Chelton. 2000. Satellite measurements of sea surface temperature through clouds. *Science* 288(5467): 847–850.

Wiseman, W., and W. Sturges. 1999. The physical oceanography of the Gulf of Mexico: processes that regulate its biology. In *The Gulf of Mexico large marine ecosystem*, ed. H. Kumpf, K. Steidinger, and K. Sherman. Malden: Blackwell Science, Inc.

Yarnal, B. 1993. *Synoptic climatology in environmental analysis: a primer*. London: Bellhaven Press. 195 pp.